High performance graphene-based pseudo-ductile composites

Mohammad Hamidul Islam,[1] Shaila Afroj,[1] and Nazmul Karim[1]*

[1]Centre for Print Research (CFPR), The University of the West of England Bristol (UWE Bristol), Frenchay, Bristol BS16 1QY, UK

Email: nazmul.karim@uwe.ac.uk

Abstract

High-performance fibre reinforced polymer (FRP) composites offer excellent specific strength and stiffness when compared to high-density metallic materials. However, their inherent brittleness leads to sudden and catastrophic failure without sufficient pre-warning, rendering them unsuitable for many applications. To address this limitation, we present a novel approach using graphene-based glass-carbon FRP hybrid composites that exhibit excellent pseudo-ductile properties. Our technique involves coating glass and carbon fibre balanced plain woven fabrics with graphene-based materials using a facile and scalable pad-dry-cure coating technique, followed by reinforcement with an epoxy matrix via vacuum-assisted resin infusion (VARI). Our tensile and flexural tests demonstrate the exceptional pseudo-ductile behaviour of these hybrid composites, with no visible changes in damage initiation after the initial failure of carbon fibre. By enabling the manufacture of high-performance pseudo-ductile composites at scale using a low-cost manufacturing method, our graphene-based glass-carbon hybrid FRP composites have significant potential for next-generation applications.

Keywords: Fibre reinforced polymer (FRP), Graphene, pseudo-ductility, and hybrid composites.

Introduction

High-performance FRP composites are widely employed in advanced lightweight engineering applications due to their remarkable mechanical properties.[1-3] However, a fundamental limitation of such composites is their inherent brittleness, which can lead to sudden and catastrophic failure without adequate pre-warning. This drawback has rendered such composites unattractive for many applications. The full potential of FRP composites in terms of their outstanding structural properties remains untapped due to concerns over their safety and potential for sudden and catastrophic failure. Therefore, the development of high-performance FRP composites with inherent ductility is critical to expanding the range and volume of applications for composite materials. While a clear definition for pseudo-ductility does not exist, this property can be quantified using the pseudo-ductile strain, which can be defined as the difference between the final failure strain and the projected elastic strain at the failure stress.[4] Numerous approaches have been employed to impart ductility in high-performance composites, enabling a gradual failure mode while maintaining high strength and specific stiffness.[5-8]

Introduction of ductile fibers, such as stainless steel, has shown to improve the failure strain of composites.[9, 10] However, the higher density of steel fibers can limit their application in weight-critical contexts by reducing the specific strength. Modification of traditional reinforced materials in composite laminates has been studied as an alternative method for generating additional strain and non-linear response during tensile loading. Additional strain and non-linear response can be achieved through various methods, including reorientation of off-axis fibers and matrix shearing through angle plies,[11, 12] excess length via out-of-plane waviness,[13, 14] highly aligned discontinuous fibers,[15, 16] or shear under tension in a biaxial braid structure.[17, 18] However, braided composites typically do not exhibit an increase in stress after the initial failure, making true pseudo-ductility unattainable with such architecture. Promising ductile fibers, such as carbon nanotubes [19] and regenerated cellulose, [20] have been identified. However, these new fibers are unable to provide elastic moduli and strength values comparable to those of traditional glass or carbon fibers, making the commercialization of ductile composites for macroscale structural applications a challenging and time-consuming process.

Hybridizing low strain (LS) to failure fibers with high strain (HS) to failure fibers is one of the most commonly used methods for achieving pseudo-ductility.[21] Fiber hybridization can be performed using various methods, such as interlayer or layer-by-layer, [22] intralayer or yarn-by-yarn,[23] and intra-yarn or fiber-by-fiber.[24] In hybrid composites with different failure strain values, achieving an appropriate fiber volume fraction (V_f) for the two different fibers is critical for producing progressive failure of the composite.[25] Recent studies have indicated that a thin-ply interlayer unidirectional (UD) hybrid architecture is a promising approach for achieving favorable ductile or pseudo-ductile behavior in

composites.[26-30] In most cases, such UD interlayer hybrid composites are produced by embedding thin carbon fiber (LS) layers between glass fiber (HS) layers to create pseudo-ductility through the progressive fragmentation of the carbon layer and delamination of the carbon/glass interface. Although thin-ply UD hybrid composites have good pseudo-ductile properties, unbalanced load-bearing capacity, higher manufacturing costs, and poor preform drapability relative to woven fabric preforms present obstacles to their industrial application.

Graphene and its derivatives have drawn sinficnat research interests in recent years as potential materials for producing multifunctional textiles[31-34] and composites,[35-37] due to superior mechanical, electrical, and thermal properties of graphene and its derivatives.[38, 39] Due to these multifunctional properties, graphene material has garnered a high level of interest for use as a filler in high-performance FRP composites.[40, 41] Graphene oxide (GO), an oxidized derivative of graphene, is formed by attaching various oxygen functional groups (e.g., hydroxyl, epoxy, and carbonyl groups) to the basal plane and edges of a graphene sheet.[42] Many studies have aimed to improve the interfacial properties of FRP composites by introducing GO in the composites through modifying resins or fibers.[43-47] Additionally, the Graphene Nanoplatets (GNP), made up of a few layers of graphene stacked together in a plate-like shape, can be produced at a relatively low cost through a top-down approach, including mechanical exfoliation and liquid-phase exfoliation from pre-treated graphite.[48] However, incorporating GNP into FRP composites is a challenging task. It is important to develop a time- and cost-effective processing technique to incorporate the GNP into FRP composites that is easier to scale up to industrial production. To date, there is no published work available on pseudo-ductility in graphene-based FRP composites, which is the focus of this study.

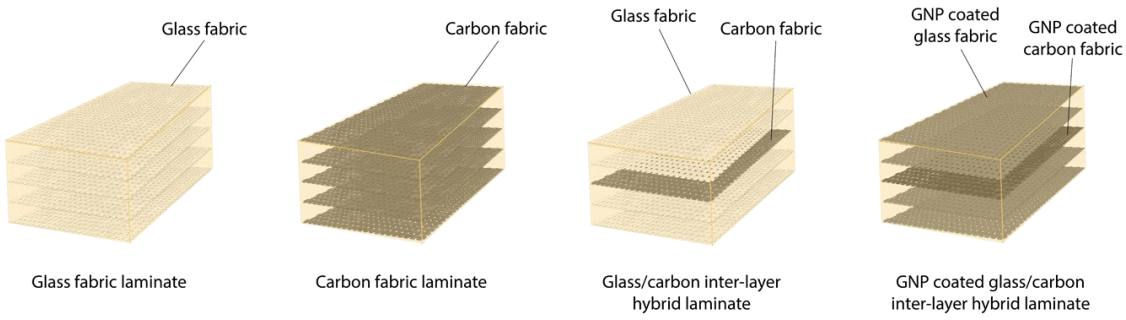

Fig. 1 Schematic of the layup process of different composites.

Here, we present a novel approach to siginifcanly enhance the pseudo-ductile behavior of GNP-coated woven glass-carbon/epoxy interlayer hybrid composites, which have the ability to bear loads in both directions and are more practical for real-life applications than UD hybrid composites. Commercially available E-glass and carbon fiber balanced fabrics were coated with GNP at different concentrations using a simple and highly scalable pad-dry-cure coating method, and the composites were

manufactured via a VARI process using four fabric lay-up configurations, as illustrated in Fig. 1. The results of tensile tests showed that glass-carbon/epoxy and GNP-coated glass-carbon/epoxy hybrid composites exhibited excellent pseudo-ductile behavior. However, the GNP-coated glass-carbon/epoxy hybrid composites showed a higher level of pseudo-ductile strain compared to the glass-carbon/epoxy hybrid composite.

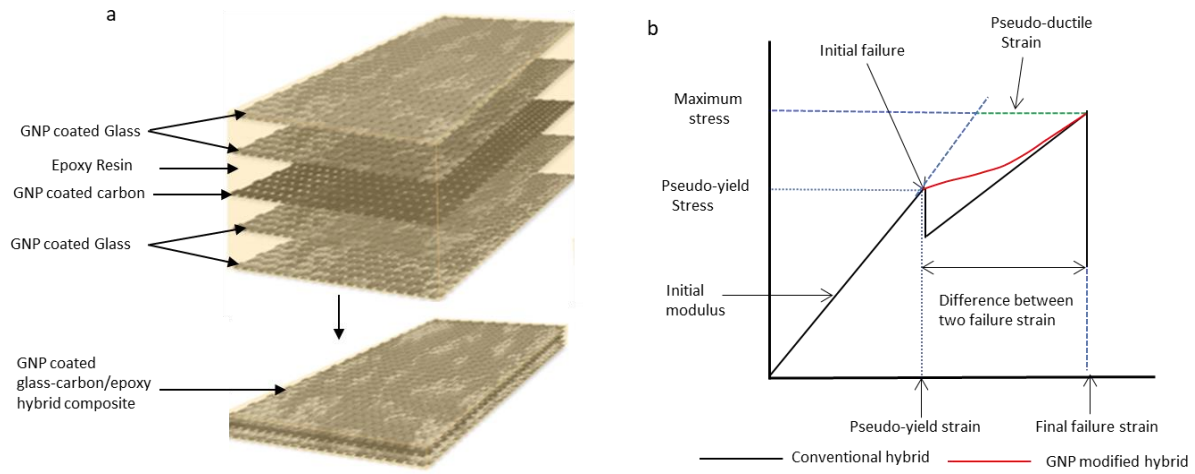

Fig. 2. a) Design of GNP-coated glass-carbon/epoxy hybrid composite and b) Schematic of the stress-strain response of conventional and GNP-coated glass-carbon/epoxy hybrid composites with the graphical representation of pseudo-ductile properties.

Results and Discussion

Design Approach

This section describes the design approach and materials used to ensure a stable pseudo-ductile failure of the hybrid composites. A previous study[26] presented an analytical method that demonstrated the importance of LS fiber fragmentation and dispersed delamination in achieving the pseudo-ductile behavior of the hybrid composites during tensile loading. Hybrid architecture and the proportion of LS and HS fibers play a crucial role in achieving LS fiber fragmentation and dispersed delamination. In addition, the thickness of LS fibers affects the pseudo-ductile behavior of the composite.[28, 29] The outer HS fiber layers must be thick and strong enough to take the full load after LS fiber failure. Another study,[25] showed that the fiber volume fraction (V_f) of two different fibers with different failure strain values is important for achieving a progressive failure of the hybrid composites. The pseudo-ductile response was only achieved using 10 to 25% of LS fibers by volume. Recent studies have shown that the incorporation of a small amount of nanofiller, such as graphene, in FRP composites could significantly improve interface-dominated properties.[49, 50] Nanofiller improves the fiber/matrix bonding, which plays a vital role in efficient stress transfer, reduces local stress concentration around the fiber-matrix interface, and improves interfacial properties.

In this study, to achieve pseudo-ductility in a hybrid composite, glass and carbon fabrics were coated with GNP. The GNP could be attached to the fabric surface, improving the fibre-matrix interactions and forming a link between the glass-carbon fibre layers. This helped to promote carbon fibre fragmentation, dispersed delamination, and stable load transfer to glass fibre after carbon fibre failure. GNP-coated glass-carbon/epoxy inter-layer hybrid composite laminates were manufactured, with one layer of carbon fabric placed in the middle of four layers of glass fabric, Fig. 2a. The glass and carbon fibre volume ratio in the composite was maintained at 90:10 to promote fragmentation of the central carbon layer and stable delamination around the fractures in the carbon layer. In this way, the typical major load drop at the fracture of the carbon fibre in the hybrid composite could be avoided, and a slightly rising plateau could be generated instead, with further rise after complete fragmentation of the carbon fibre. A schematic of the stress-strain response of conventional and GNP-coated glass-carbon/epoxy hybrid composites with graphical representation of pseudo-ductile properties is shown in Fig. 2b.

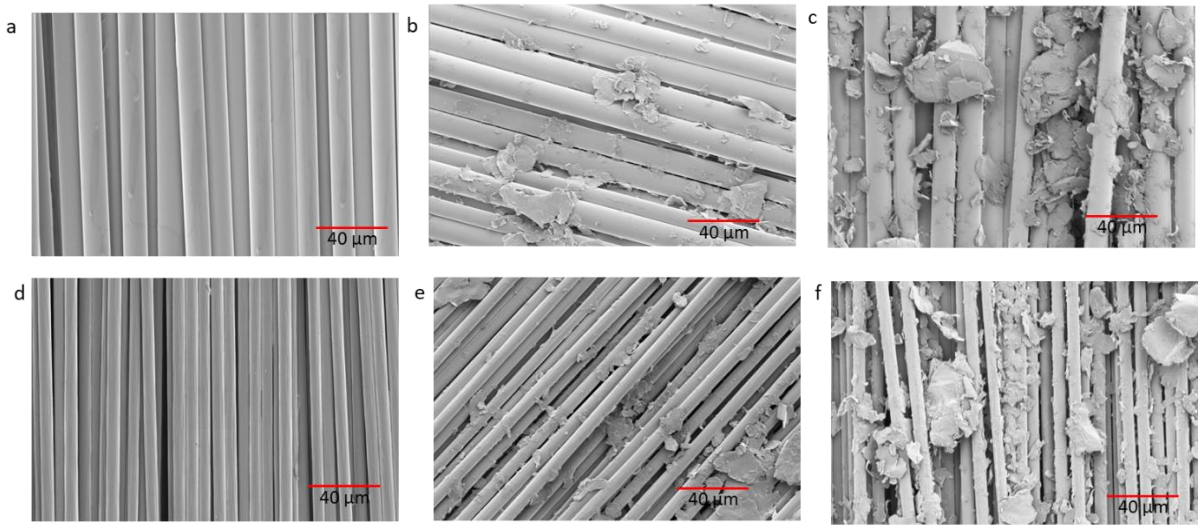

Fig. 3. SEM images of a) untreated glass fabric (X1000); b) 1 wt.% GNP-coated glass fabric (X1000), c) 5 wt.% GNP-coated glass fabric (X1000), d) untreated carbon fabric (X1000); e) 1 wt.% GNP-coated carbon fabric (X1000), and f) 5 wt.% GNP-coated carbon fabric (X1000).

Characterization of GNP-coated glass and carbon fabric

A highly scalable pad-dry-cure coating technique was used to coat glass and carbon fibre fabrics with GNP at two different concentrations. This process can coat fabrics at a very high speed of ~150 m/min [51, 52]. The SEM images of uncoated and GNP-coated glass and carbon fibre fabrics with different GNP concentrations are shown in Fig. 3a-f. The surfaces of uncoated glass and carbon fibres are smooth and clean (Fig. 3a and d). After coating with GNP, the surface roughness of coated fibres is noticeable,

as seen from Fig. 3b-c and e-f, which may be due to the fact that GNP is attached to the fibre surface by mechanical interlocking. As seen in Fig. 3b-c and e-f, GNP flakes were randomly distributed on glass and carbon fibre surfaces with some aggregated GNP in some areas. Aggregation occurs more for 5 wt.% GNP-coated fibre surface (Fig. 3c and f) compared to the 1 wt.% GNP-coated glass fibre surface (Fig. 3b and e).

Table 1. Tensile test results of different composites laminates

Composites	**Pseudo-yield stress (MPa)**	**Maximum Stress (MPa)**	**Initial Modulus (GPa)**	**Pseudo-yield strain (%)**	**Ultimate failure strain (%)**	**Difference between Initial and ultimate failure strain (%)**
Carbon/epoxy		567.9±16.6	49.7±1.65		1.29±0.07	
Glass/epoxy		454.0±7.2	18.9±1.8		3.26±0.13	
Glass-carbon/epoxy	302.7±11.9	344.4±14.2	21.7±1.1	1.56±0.06	2.08±0.08	0.52±0.09
1 wt.% GNP-glass-carbon/epoxy	372.0±10.3	408.2±11.8	25.4±0.7	1.53±0.05	2.26±0.11	0.73±0.09
5 wt.% GNP-glass-carbon/epoxy	344.8±10	377.9±12.2	24.2±1.4	1.56±0.04	2.74±0.21	1.18±0.25

Tensile properties

Three different types of hybrid composite laminates were prepared from untreated and GNP-coated glass and carbon fabrics, and epoxy resin. Two concentrations (1 and 5 wt.%) of GNP dispersion were used to coat the fabric. Glass/epoxy and carbon/epoxy composites were also manufactured for baseline specimens. Tensile test results of different composites are presented in Table 1.

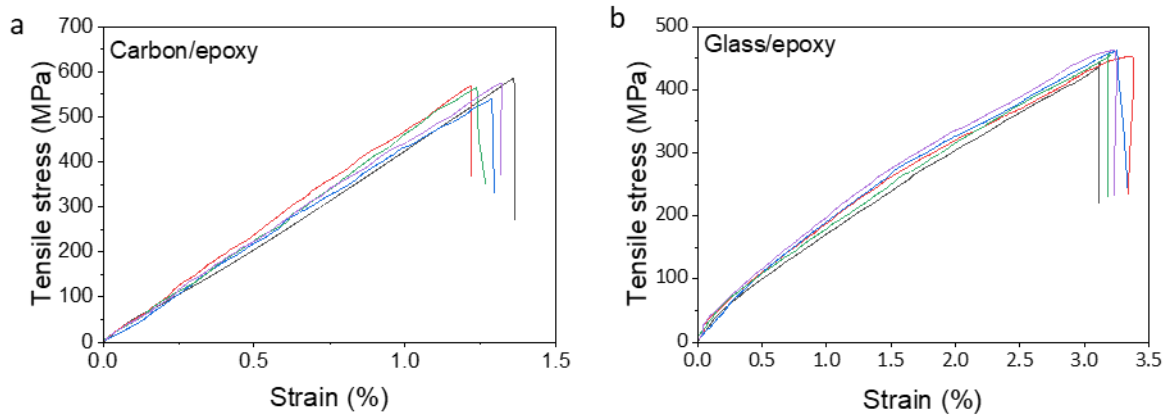

Fig. 4. Tensile stress-strain graph of a) carbon/epoxy and b) glass/epoxy composite.

Fig. 4 shows the tensile stress-strain response of the neat carbon/epoxy and glass/epoxy composites laminates. Both carbon and glass fabric composites show a catastrophic failure. The tensile stress of the glass and carbon fibre composites was found to be ~454 and ~568 MPa, and the tensile strain was found to be ~3.26 and ~1.29%, respectively. Stress-strain responses of untreated glass-carbon/epoxy and GNP-coated glass-carbon/epoxy hybrid composites are shown in Fig. 5a-c. Images at different strain levels during the tensile tests (recorded using a high-speed video camera) are also shown on the right side of the respective graphs (i-iv). All the hybrid composites demonstrate non-linearity in their stress-strain graph instead of a sudden catastrophic failure. There was no load drop after the initial failure of the carbon layer, and a smooth transition of stress after carbon fibre failure was observed. As carbon fibre has a lower strain to failure compared to that of glass, therefore carbon fibres failed initially. Once the carbon fibres failed, the stress was redistributed to the high-strain glass fibres that carried the load to ultimate failure. A significant variation of the pseudo-ductile properties of GNP-coated glass-carbon/epoxy hybrid composites was observed compared to untreated glass-carbon/epoxy hybrid composite.

The graph shows a noticeable change in slope in the hybrid composites after the pseudo-yield point where the carbon layer failed and the fragmentation of carbon fibre took place. However, there was not enough stress and strain value after the initial failure for the glass-carbon/epoxy composite. The fragmentation of the carbon layer and crack propagation were visible in the specimen and progressively covered the whole specimen (Fig.5a-ii-iii). However, there were no visible changes on the specimen surfaces observed for GNP-coated glass-carbon/epoxy composite after initial failure (Fig. 5b-ii and 5c-ii). Some changes were observed on the specimen surfaces before ultimate failure (Fig. 5b-iii and 5c-iii). The pseudo-yield strain of untreated and GNP-coated hybrid composites was between ∼1.53% to ∼1.56%, which is higher than the pure carbon fibre fabric composite failure strain (∼1.26%). These results indicated that the hybrid effect occurred in all glass/carbon hybrid composites. A previous study reported an enhancement in the strain at failure of LS material up to 20% for very thin plies glass/carbon hybrid composite.[22]

The effect of GNP coating on the pseudo-ductile properties of GNP-glass-carbon/epoxy composites with different GNP concentrations is shown in Fig. 5b-c. Both 1 and 5 wt.% GNP-coated glass-carbon/epoxy hybrid composites showed an excellent pseudo-ductile response during tensile loading. A significant difference in the failure behaviour of the 1 wt.% GNP-coated glass-carbon/epoxy hybrid composite compared to the 5 wt.% GNP-coated glass-carbon/epoxy hybrid composite was observed. The pseudo-yield stress and initial modulus of these composites were higher compared to uncoated glass-carbon/epoxy hybrid composites. The pseudo-yield stress of 1 and 5 wt.% GNP-coated composites was increased by ∼22.89% and ∼13.90%, respectively, compared to uncoated glass-

carbon/epoxy hybrid composites. The highest modulus and maximum stress values were achieved with 1 wt.% GNP-coated glass-carbon/epoxy hybrid composites. Young's modulus increased by ~17.05% and ~11.52%, and ultimate failure stress increased by ~18.52% and ~9.72%, respectively, for 1 and 5 wt.% GNP-coated composites compared to that of glass-carbon/epoxy hybrid composite. However, the ultimate failure strain of 5 wt.% GNP-coated composite was higher than untreated and 1 wt.% GNP-coated composite (Table 1).

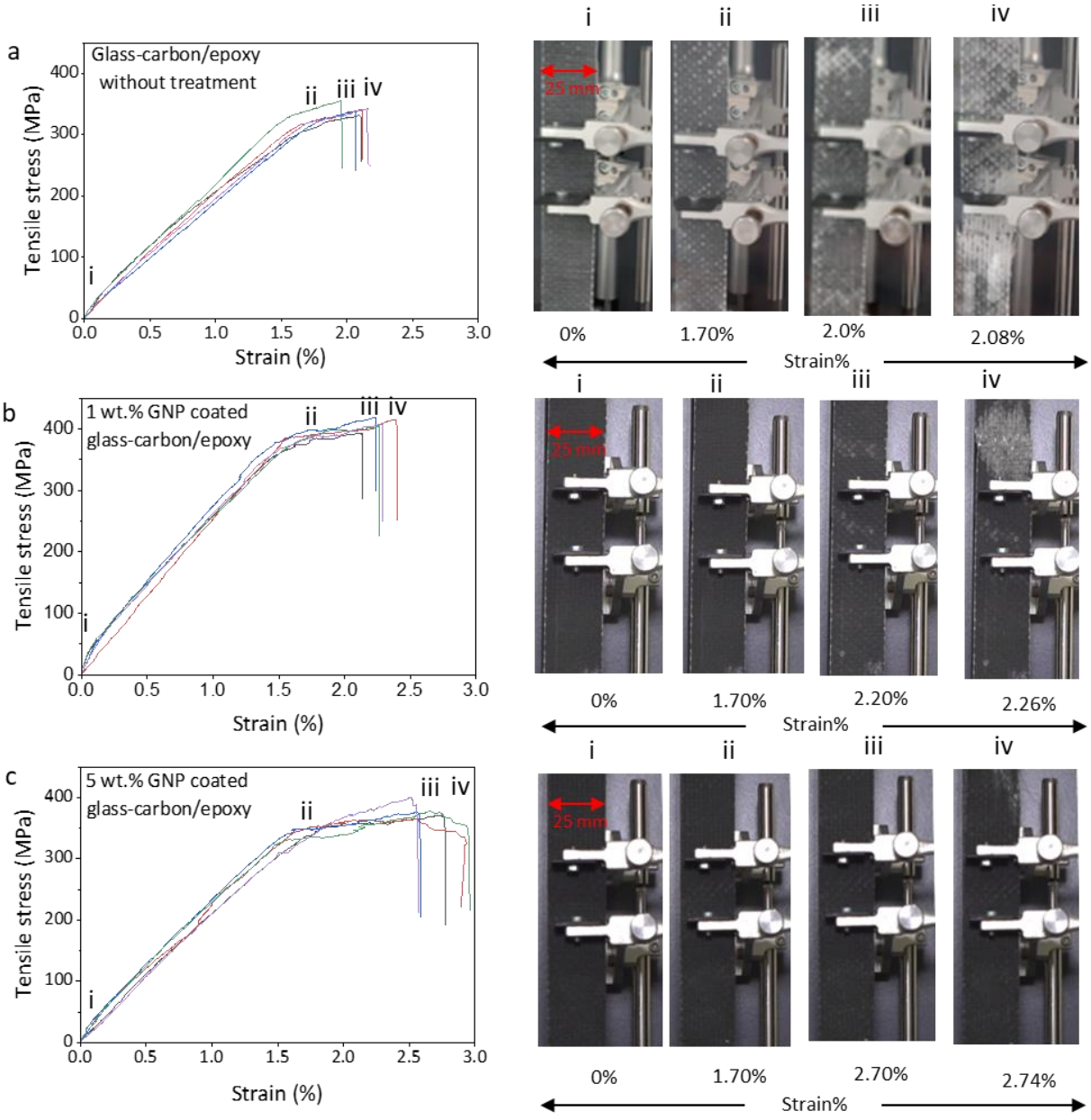

Fig. 5. Tensile stress-strain graph of a) glass-carbon/epoxy hybrid, b) 1 wt.% GNP-coated glass-carbon/epoxy hybrid and c) 5 wt.% GNP coated glass-carbon/epoxy hybrid composite. Images of specimens at different strain levels i) start, ii) after the initial failure, iii) just before ultimate failure and iv) after ultimate failure.

In glass-carbon/epoxy hybrid composites, crack initiation occurs after carbon fibre failure at the matrix site and spreads rapidly due to the absence of mechanical interlocking between the fibres and matrix. The crack starts to propagate at the matrix along the fibre axis, and delamination occurs between different fibre layers (Fig. 5a ii-iii). However, in GNP-coated glass-carbon/epoxy hybrid composites, the GNP on the fabric surface acts as a bridge, increasing the mechanical interaction between fibres and matrix. This formed a stronger graphene-epoxy matrix interface.[53] Due to this strong interface among the GNP-fibre and epoxy chain, the tensile strength of the GNP-coated glass-carbon/epoxy hybrid composite was enhanced. The strong interface of the graphene nanoplatelets can act as a bridging element that reduces stress concentration and delays crack propagation in the interface region, promoting a smooth transfer of load from the carbon to the glass fibres after initial failure. [46, 47, 54].

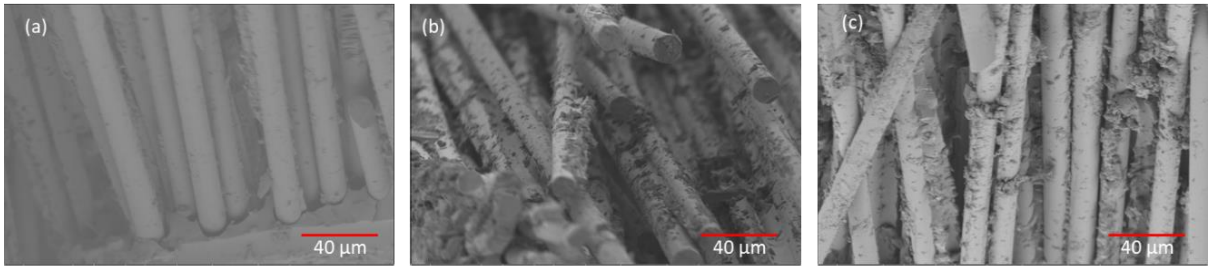

Fig. 6. SEM micrographs of the fracture surfaces after the tensile test a) glass-carbon/epoxy without coating, b) 1 wt.% GNP coated glass-carbon/epoxy and c) 5 wt.% GNP coated glass-carbon/epoxy composites.

The fracture surface morphology of the composites was analysed after the tensile test using SEM. Fig. 6a shows the fracture surface image of the glass-carbon/epoxy hybrid composite without coating, while Fig. 6b-c shows the GNP-coated glass-carbon/epoxy hybrid composites of 1 wt.% and 5 wt.% GNP, respectively. The without-coating glass-carbon/epoxy shows a smooth fracture surface, indicating relatively brittle failure. However, the GNP-coated glass-carbon/epoxy composite shows a relatively rougher surface compared to the uncoated composite. These results indicate that the GNP is mechanically interlocking with the fibre, which suppresses the crack propagation after the initial failure of the carbon fibre and transfers the load to the glass fibre.

2.2 Flexural properties

To investigate the effect of GNP coating on the flexural properties of different composites, 3 points bending test was performed. The summary of the flexural test results of different composites laminate is presented in Table 2.

Table 2 Flexural test results of different composites laminates

Composites	**Maximum Stress (MPa)**	**Modulus (GPa)**	**Peak strain (%)**
Carbon/epoxy	732.8 ± 31.3	38.6 ± 0.22	2.04 ± 0.02
Glass/epoxy	379.9 ± 17.3	16.0± 0.10	3.49 ± 0.10
Glass-carbon/epoxy	374.9 ± 5.3	16.7 ± 0.10	3.08 ± 0.19
1 wt.% GNP-glass-carbon/epoxy	420.2 ± 13.5	17.6 ± 0.08	3.90 ± 0.12
5 wt.% GNP-glass-carbon/epoxy	396.9 ± 5.1	17.8 ± 0.05	3.17 ± 0.23

Fig. 7 shows the flexural stress-strain graph of the glass-carbon/epoxy and GNP-coated glass-carbon/epoxy composites with different GNP concentrations. The glass-carbon/epoxy and GNP-coated glass-carbon/epoxy hybrid composites with different GNP concentrations exhibit different flexural properties and failure behavior. It is noteworthy that all the stress-strain curves rise linearly during the early loading stage (up to 2.25% strain) and show some nonlinearity before ultimate failure. However, after a certain strain (~3%), the GNP-coated composite behaves differently than the non-coated specimen. Pseudo-ductile behavior is also observed in the flexural stress-strain graphs for all hybrid composites. The GNP-coated composites demonstrated larger stress-strain values before ultimate failure. The flexural stress of the glass-carbon/epoxy composite was found to be ~374.9 MPa. At 1% and 5 wt.% GNP coated glass-carbon/epoxy composites, the flexural stress was found to be ~420.2 and ~396.9 MPa, respectively, which are ∼12.1% and ∼6% higher compared with that of the glass-carbon/epoxy composite. The increment of flexural stress with the 5% GNP coated composite was less pronounced in comparison with that of the 1% GNP coated composite. This might be due to the agglomeration of GNP at the interfacial region, which generates stress concentration and hence reduces the strength at the interface. A higher flexural strain of ~3.9% was observed with 1 wt.% GNP coated glass-carbon/epoxy composite, which is approximately 26.6% higher compared to the control specimen. This enhancement of flexural stress and strain with GNP coated glass-carbon/epoxy composites is likely due to the wrinkled structure of GNP that is attached to the fibre surface by mechanical interlocking, which improves the fibre matrix interactions and forms a link between the glass-carbon fibre layer. Therefore, the strong GNP/fibre/matrix interfacial interactions created from

the randomly distributed GNP at the interface facilitate smooth load transfer to glass fibre after carbon fibre failure, thus contributing to higher flexural stress and strain as well as pseudo-ductility.

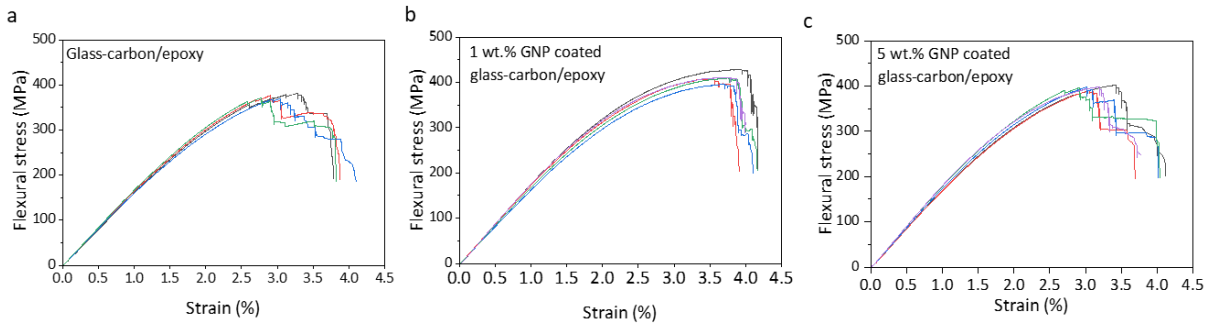

Fig. 7. Flexural stress-strain graph of a) glass-carbon/epoxy, b) 1 wt.% GNP coated glass-carbon/epoxy and c) 5 wt.% GNP coated glass-carbon/epoxy composite.

Conclusion

In this study, we report graphene-based glass-carbon/epoxy interlayer hybrid composites with excellent pseudo-ductile properties. GNP was incorporated into the glass and carbon fabric using a highly scalable pad-dry-cure coating method. Microstructural investigation revealed that GNP was randomly distributed onto the glass and carbon fibre surface. Both 1 and 5 wt.% GNP-coated glass-carbon/epoxy hybrid composites exhibited excellent pseudo-ductility during tensile loading. The 1 wt.% GNP-coated glass-carbon/epoxy hybrid composite demonstrates higher strength and modulus compared to the 5 wt.% GNP-coated glass-carbon/epoxy hybrid composite. However, the 5 wt.% GNP-coated glass-carbon/epoxy hybrid composite shows a higher pseudo-ductile strain. The excellent pseudo-ductility of the resulting composites can be attributed to the GNP that is distributed on the fibre surface improving the fibre-matrix interfacial interaction by mechanical interlocking, which facilitated smooth load transfer from the carbon to the glass fibre after carbon fibre failure. The graphene-based glass/carbon hybrid composite could be a suitable approach to manufacturing high-performance pseudo-ductile composites for structural applications.

Experimental

Materials

Commercial E-glass fiber and Toray carbon fiber plain woven fabrics were purchased from Easy Composites, UK. The areal weight of the glass fabric was approximately ~290 g/m² with a weave density of 4 ends and picks per cm. The areal weight of the carbon fiber fabric was approximately ~90 g/m² with a weave density of 7 ends and picks per cm. EL2 epoxy laminating resin and AT30 slow

hardener were purchased from Easy Composites, UK. Araldite 2011 A/B epoxy adhesive was purchased from Huntsman, USA. 2-Propanol (≥99.5%) was purchased from Sigma-Aldrich, UK. Graphene nanoplatelets (GNP) (xGNP, Grade M-15, XG Science, Lansing USA) with a nominal lateral size of approximately ~15 µm as reported by the supplier were used. The manufacturer reported that the average thicknesses of all the flakes were in the range of approximately ~6–8 nm.

Preparation of GNP dispersion

GNP dispersions were prepared using a bath-type sonication method. Since they do not disperse in water without a surfactant, GNPs (1 and 5 wt.%) were dispersed in 2-propanol (IPA) and deionized water (DI) (50% propanol + 50% water) to prepare a homogeneous dispersion. Firstly, the GNP, IPA, and DI water were mixed using a magnetic stirrer for 2 hours. Then, the GNP dispersion was sonicated in a bath sonicator for 2 hours to achieve a homogeneous dispersion.

Coating of glass and carbon fabric

Both the glass and carbon fibre fabrics were cut into dimensions of 300 mm × 250 mm. The pad-dry-cure coating technique (as shown in Fig. 8) was employed to coat the glass and carbon fibre fabrics with GNP dispersion. A laboratory-scale padder machine (Roaches, UK) was used to coat the glass and carbon fabrics with the GNP dispersion, followed by drying at 100°C for 7 minutes in a Mini-Thermo (Roaches, UK). The GNP ink was placed between the two rubber rollers of the padder, and the padding roller pressure and speed were adjusted to 0.5 bar and 1 m/min, respectively. Two coating cycles were carried out, with each cycle including one padding and one drying pass.

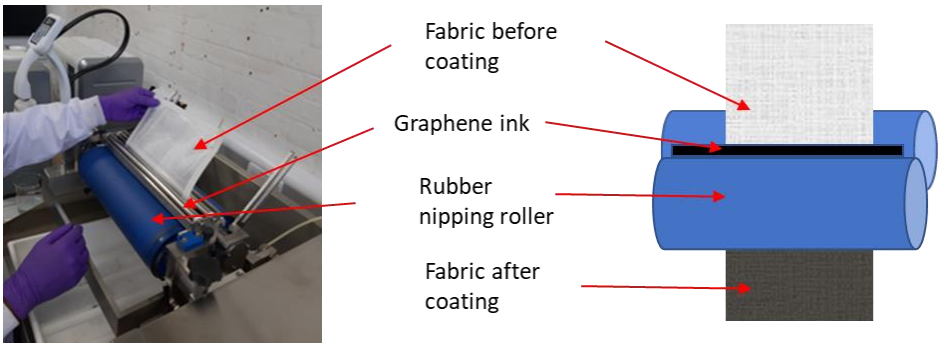

Fig. 8. Photograph and schematic of the fabric coating process.

Table 3 List of the different laminates

Laminate configurations	Lay-up sequences	GF areal density (g/m^2)	CF areal density (g/m^2)	Volume of HS fibre (%)	Volume of LS fibre (%)
Glass fibre	5L G	290	-	100%	
Carbon fibre	5 L C	-	90	-	100%
Glass/carbon	2L G +1L C+ 2LG	290	90	90	10
GNP coated glass and carbon (2 laminates at different GNP concentrations)	2L G +1L C+ 2LG	290	90	90	10

Composite manufacturing

GNP coated glass-carbon/epoxy inter-layer hybrid composite laminates were manufactured using a VARI process. To compare the performance of hybrid composites with the baseline materials, glass/epoxy, carbon/epoxy and glass-carbon/epoxy inter-layer hybrid composite laminates were also manufactured. Five types of composites were fabricated for the current investigation, and each composite contains five layers of fabric. The hybrid composites consist of four layers of glass and one layer of carbon fabric. The lay-up sequence was two layers of glass, one layer of carbon and then two layers of glass fabrics. The ratio of glass to carbon fibre by volume in the composites was 90:10. The schematic diagram of the stacking sequence of glass, carbon and glass/carbon hybrid composites is shown in Fig. 2. A peel ply was used on the bottom and top side of the layered fabric to ensure easy de-molding of composites. In addition, a mesh fabric was also placed on top to ensure an even flow of resin during the infusion process. The preform was sealed by a plastic bag and vacuum pressed using a pump. EL2 epoxy laminating resin and AT30 slow epoxy hardener were degassed separately for 1 h and then mixed together. The mixed resin was again de-gassed for 30 min to ensure there were no bubbles inside the resin. Finally, the resin is carefully sucked into the preform through the resin inlet and outlet tube using a vacuum pump. The resin-infused preforms were cured at room temperature for 48 h. Five different types of composite laminates were manufactured, and the list of laminates is presented in Table 3.

Characterization

The surface topography of the untreated and GNP-coated glass and carbon fibre fabrics was analysed using an FEI Quanta 650 Field Emission Scanning Electron Microscope (SEM). After the tensile test, the fracture specimens were also observed under SEM to observe the GNP-coated fibre matrix interaction.

To avoid charging, all the specimens were gold-coated using an Emscope SC500 gold sputter coating unit before the SEM analysis.

Tensile strength testing of composites

All the composite specimens were prepared for tensile testing according to ASTM D3039M standard. Five specimens (250 mm long and 25 mm wide) were prepared for each type of composite for tensile testing. End tabs made of glass fibre reinforced cross-ply plates with a thickness of 1.60 mm were bonded to the specimen using Araldite 2011 A/B epoxy adhesive mixer. The individual samples were cut from the composite panel with a diamond cutting wheel. Tensile tests were carried out using a Testometric X350-20 (UK) tensile testing machine, which was equipped with a 20 kN load cell at a crosshead speed of 2 mm/min. The strain was measured using a mechanical extensometer with a nominal gauge length of 25 mm. A high-speed video camera (Sony HXR-NX 80) was used for in-situ observation during the test.

Flexural test

The flexural tests were performed according to the ASTM D-790 standard. The dimensions of the test specimens used were 74 mm in length, 13 mm in width, and 1.1 mm in thickness. The span-to-depth ratio was set to 40:1. Flexural tests were carried out using a Testometric X350-20 (UK) testing machine, which was equipped with a 20 kN load cell at a crosshead speed of 1 mm/min. At least five specimens were tested for each composite sample.

Corresponding author

All the correspondence should be addressed to nazmul.karim@uwe.ac.uk

Acknowledgments

The authors acknowledge UKRI Expanding Excellence in England (E3) funding from Research England.

References

1. Yang, G.; Park, M.; Park, S.-J., Recent progresses of fabrication and characterization of fibers-reinforced composites: A review. *Composites Communications* **2019,** *14*, 34-42.
2. Maiti, S.; Islam, M. R.; Uddin, M. A.; Afroj, S.; Eichhorn, S. J.; Karim, N., Sustainable Fiber-Reinforced Composites: A Review. *Advanced Sustainable Systems* **2022,** *6* (11), 2200258.
3. Sarker, F.; Potluri, P.; Afroj, S.; Koncherry, V.; Novoselov, K. S.; Karim, N., Ultrahigh Performance of Nanoengineered Graphene-Based Natural Jute Fiber Composites. *ACS Applied Materials & Interfaces* **2019,** *11* (23), 21166-21176.
4. Wisnom, M. R.; Czél, G.; Fuller, J. D.; Jalalvand, M., High performance pseudo-ductile composites. *20th International Conference on Composite Materials Copenhagen* **2015,** (July), 3-7.
5. Sherman, D.; Lemaitre, J.; Leckie, F. A., The mechanical behavior of an alumina carbon/epoxy laminate. *Acta Metallurgica et Materialia* **1995,** *43* (12), 4483-4493.

6. Czél, G.; Rev, T.; Jalalvand, M.; Fotouhi, M.; Longana, M. L.; Nixon-Pearson, O. J.; Wisnom, M. R., Pseudo-ductility and reduced notch sensitivity in multi-directional all-carbon/epoxy thin-ply hybrid composites. *Composites Part A: Applied Science and Manufacturing* **2018,** *104*, 151-164.
7. Fotouhi, M.; Suwarta, P.; Tabatabaeian, A.; Fotouhi, S.; Jenkin, R.; Jalalvand, M.; Wisnom, M. R., Investigating the fatigue behaviour of quasi-isotropic pseudo-ductile thin-ply carbon/glass epoxy hybrid composites. *Composites Part A: Applied Science and Manufacturing* **2022,** *163*, 107206.
8. Ichenihi, A.; Li, W.; Gao, Y.; Rao, Y., Feature selection and clustering of damage for pseudo-ductile unidirectional carbon/glass hybrid composite using acoustic emission. *Applied Acoustics* **2021,** *182*, 108184.
9. Allaer, K.; De Baere, I.; Lava, P.; Van Paepegem, W.; Degrieck, J., On the in-plane mechanical properties of stainless steel fibre reinforced ductile composites. *Composites Science and Technology* **2014,** *100*, 34-43.
10. Callens, M. G.; Gorbatikh, L.; Verpoest, I., Ductile steel fibre composites with brittle and ductile matrices. *Composites Part A: Applied Science and Manufacturing* **2014,** *61*, 235-244.
11. Fuller, J. D.; Wisnom, M. R., Pseudo-ductility and damage suppression in thin ply CFRP angle-ply laminates. *Composites Part A: Applied Science and Manufacturing* **2015,** *69*, 64-71.
12. Yuan, Y.; Wang, S.; Yang, H.; Yao, X.; Liu, B., Analysis of pseudo-ductility in thin-ply carbon fiber angle-ply laminates. *Composite Structures* **2017,** *180*, 876-882.
13. Diao, H.; Robinson, P.; Wisnom, M. R.; Bismarck, A., Unidirectional carbon fibre reinforced polyamide-12 composites with enhanced strain to tensile failure by introducing fibre waviness. *Composites Part A: Applied Science and Manufacturing* **2016,** *87*, 186-193.
14. Pimenta, S.; Robinson, P., Wavy-ply sandwich with composite skins and crushable core for ductility and energy absorption. *Composite Structures* **2014,** *116*, 364-376.
15. Czél, G.; Jalalvand, M.; Wisnom, M. R., Demonstration of pseudo-ductility in unidirectional hybrid composites made of discontinuous carbon/epoxy and continuous glass/epoxy plies. *Composites Part A: Applied Science and Manufacturing* **2015,** *72*, 75-84.
16. Finley, J. M.; Yu, H.; Longana, M. L.; Pimenta, S.; Shaffer, M. S. P.; Potter, K. D., Exploring the pseudo-ductility of aligned hybrid discontinuous composites using controlled fibre-type arrangements. *Composites Part A: Applied Science and Manufacturing* **2018,** *107*, 592-606.
17. Del Rosso, S.; Iannucci, L.; Curtis, P. T., Experimental investigation of the mechanical properties of dry microbraids and microbraid reinforced polymer composites. *Composite Structures* **2015,** *125*, 509-519.
18. Gautam, M.; Sivakumar, S.; Barnett, A.; Barbour, S.; Ogin, S. L.; Potluri, P., On the behaviour of flattened tubular Bi-axial and Tri-axial braided composites in tension. *Composite Structures* **2021,** *261*, 113325.
19. Boncel, S.; Sundaram, R. M.; Windle, A. H., Enhancement of the Mechanical Properties of Directly Spun CNT Fibres by Chemical Treatment. *ACS nano* **2011,** *5* (12), 9339-9344.
20. Shamsuddin, S.-R.; Lee, K.-Y.; Bismarck, A., Ductile unidirectional continuous rayon fibre-reinforced hierarchical composites. *Composites Part A: Applied Science and Manufacturing* **2016,** *90*, 633-641.
21. Swolfs, Y.; Gorbatikh, L.; Verpoest, I., Fibre hybridisation in polymer composites: A review. *Composites Part A: Applied Science and Manufacturing* **2014,** *67*, 181-200.
22. Wisnom, M. R.; Czél, G.; Swolfs, Y.; Jalalvand, M.; Gorbatikh, L.; Verpoest, I., Hybrid effects in thin ply carbon/glass unidirectional laminates: accurate experimental determination and prediction. *Composites Part A: Applied Science and Manufacturing* **2016,** *88*, 131-139.
23. Ikbal, H.; Wang, Q.; Azzam, A.; Li, W., Effect of hybrid ratio and laminate geometry on compressive properties of carbon/glass hybrid composites. *Fibers and Polymers* **2016,** *17* (1), 117-129.
24. Islam, M. H.; Koncherry , V.; Wisnom, M.; Potluri, P. In *Pseudo-ductile Composites with Micro-wrapped Hybrid Tow*, Proceedings of the American Society for Composites—Thirty-third Technical Conference, 2018.

25. Tavares, R. P.; Melro, A. R.; Bessa, M. A.; Turon, A.; Liu, W. K.; Camanho, P. P., Mechanics of hybrid polymer composites: analytical and computational study. *Computational Mechanics* **2016,** *57* (3), 405-421.
26. Jalalvand, M.; Czél, G.; Wisnom, M. R., Damage analysis of pseudo-ductile thin-ply UD hybrid composites – A new analytical method. *Composites Part A: Applied Science and Manufacturing* **2015,** *69*, 83-93.
27. Fotouhi, M.; Jalalvand, M.; Wisnom, M. R., High performance quasi-isotropic thin-ply carbon/glass hybrid composites with pseudo-ductile behaviour in all fibre orientations. *Composites Science and Technology* **2017,** *152*, 101-110.
28. Czél, G.; Jalalvand, M.; Wisnom, M. R., Design and characterisation of advanced pseudo-ductile unidirectional thin-ply carbon/epoxy– glass/epoxy hybrid composites. *Composite Structures* **2016,** *143*, 362-370.
29. Jalalvand, M.; Czél, G.; Wisnom, M. R., Numerical modelling of the damage modes in UD thin carbon/glass hybrid laminates. *Composites Science and Technology* **2014,** *94*, 39-47.
30. Czél, G.; Jalalvand, M.; Wisnom, M. R.; Czigány, T., Design and characterisation of high performance, pseudo-ductile all-carbon/epoxy unidirectional hybrid composites. *Composites Part B: Engineering* **2017,** *111*, 348-356.
31. Karim, N.; Afroj, S.; Leech, D.; Abdelkader, A. M., Flexible and Wearable Graphene-Based E-Textiles. In *Oxide Electronics*, 2021; pp 21-49.
32. Islam, M. R.; Afroj, S.; Beach, C.; Islam, M. H.; Parraman, C.; Abdelkader, A.; Casson, A. J.; Novoselov, K. S.; Karim, N., Fully printed and multifunctional graphene-based wearable e-textiles for personalized healthcare applications. *iScience* **2022,** *25* (3), 103945.
33. Tan, S.; Afroj, S.; Li, D.; Islam, M. R.; Wu, J.; Cai, G.; Karim, N.; Zhao, Z., Highly sensitive and extremely durable wearable e-textiles of graphene/carbon nanotube hybrid for cardiorespiratory monitoring. *iScience* **2023,** *26* (4), 106403.
34. Tan, S.; Islam, M. R.; Li, H.; Fernando, A.; Afroj, S.; Karim, N., Highly Scalable, Sensitive and Ultraflexible Graphene-Based Wearable E-Textiles Sensor for Bio-Signal Detection. *Advanced Sensor Research* **2022,** *1* (1), 2200010.
35. Papageorgiou, D. G.; Li, Z.; Liu, M.; Kinloch, I. A.; Young, R. J., Mechanisms of mechanical reinforcement by graphene and carbon nanotubes in polymer nanocomposites. *Nanoscale* **2020,** *12* (4), 2228-2267.
36. Mohan, V. B.; Lau, K.-t.; Hui, D.; Bhattacharyya, D., Graphene-based materials and their composites: A review on production, applications and product limitations. *Composites Part B: Engineering* **2018,** *142*, 200-220.
37. Zhu, J.; Abeykoon, C.; Karim, N., Investigation into the effects of fillers in polymer processing. *International Journal of Lightweight Materials and Manufacture* **2021,** *4* (3), 370-382.
38. Lee, C.; Wei, X.; Kysar, J. W.; Hone, J., Measurement of the elastic properties and intrinsic strength of monolayer graphene. *science* **2008,** *321* (5887), 385-388.
39. Du, X.; Skachko, I.; Barker, A.; Andrei, E. Y., Approaching ballistic transport in suspended graphene. *Nature nanotechnology* **2008,** *3* (8), 491-495.
40. Wijerathne, D.; Gong, Y.; Afroj, S.; Karim, N.; Abeykoon, C., Mechanical and thermal properties of graphene nanoplatelets-reinforced recycled polycarbonate composites. *International Journal of Lightweight Materials and Manufacture* **2023,** *6* (1), 117-128.
41. Sarker, F.; Karim, N.; Afroj, S.; Koncherry, V.; Novoselov, K. S.; Potluri, P., High-Performance Graphene-Based Natural Fiber Composites. *ACS Applied Materials & Interfaces* **2018,** *10* (40), 34502-34512.
42. Singh, V.; Joung, D.; Zhai, L.; Das, S.; Khondaker, S. I.; Seal, S., Graphene based materials: Past, present and future. Elsevier Ltd: 2011; Vol. 56, pp 1178-1271.
43. Mahmood, H.; Tripathi, M.; Pugno, N.; Pegoretti, A., Enhancement of interfacial adhesion in glass fiber/epoxy composites by electrophoretic deposition of graphene oxide on glass fibers. *Composites Science and Technology* **2016,** *126*, 149-157.

44. Deng, C.; Jiang, J.; Liu, F.; Fang, L.; Wang, J.; Li, D.; Wu, J., Effects of electrophoretically deposited graphene oxide coatings on interfacial properties of carbon fiber composite. *Journal of Materials Science* **2015,** *50* (17), 5886-5892.
45. Zhang, R. L.; Gao, B.; Du, W. T.; Zhang, J.; Cui, H. Z.; Liu, L.; Ma, Q. H.; Wang, C. G.; Li, F. H., Enhanced mechanical properties of multiscale carbon fiber/epoxy composites by fiber surface treatment with graphene oxide/polyhedral oligomeric silsesquioxane. *Composites Part A: Applied Science and Manufacturing* **2016,** *84*, 455-463.
46. Sarker, F.; Potluri, P.; Afroj, S.; Koncherry, V.; S. Novoselov, K.; Karim, N., Ultrahigh Performance of Nanoengineered Graphene-Based Natural Jute Fiber Composites. *ACS Applied Materials & Interfaces* **2019,** *11* (23), 21166-21176.
47. Karim, N.; Sarker, F.; Afroj, S.; Zhang, M.; Potluri, P.; Novoselov, K. S., Sustainable and Multifunctional Composites of Graphene-Based Natural Jute Fibers. *Advanced Sustainable Systems* **2021**, 2000228.
48. Dimiev, A. M.; Ceriotti, G.; Metzger, A.; Kim, N. D.; Tour, J. M., Chemical Mass Production of Graphene Nanoplatelets in ~100% Yield. *ACS Nano* **2016,** *10* (1), 274-279.
49. Wang, F.; Cai, X., Improvement of mechanical properties and thermal conductivity of carbon fiber laminated composites through depositing graphene nanoplatelets on fibers. *Journal of Materials Science* **2019,** *54* (5), 3847-3862.
50. Wang, X.; Li, C.; Chi, Y.; Piao, M.; Chu, J.; Zhang, H.; Li, Z.; Wei, W., Effect of Graphene Nanowall Size on the Interfacial Strength of Carbon Fiber Reinforced Composites. *Nanomaterials (Basel)* **2018,** *8* (6).
51. Karim, N.; Afroj, S.; Tan, S.; He, P.; Fernando, A.; Carr, C.; Novoselov, K. S., Scalable Production of Graphene-Based Wearable E-Textiles. *ACS Nano* **2017,** *11* (12), 12266-12275.
52. Afroj, S.; Tan, S.; Abdelkader, A. M.; Novoselov, K. S.; Karim, N., Highly conductive, scalable, and machine washable graphene-based E-textiles for multifunctional wearable electronic applications. *Advanced Functional Materials* **2020,** *30* (23), 2000293.
53. Li, Y.; Zhang, H.; Huang, Z.; Bilotti, E.; Peijs, T., Graphite Nanoplatelet Modified Epoxy Resin for Carbon Fibre Reinforced Plastics with Enhanced Properties. *Journal of Nanomaterials* **2017,** *2017*, 10.
54. Seretis, G. V.; Theodorakopoulos, I. D.; Manolakos, D. E.; Provatidis, C. G., Effect of sonication on the mechanical response of graphene nanoplatelets/glass fabric/epoxy laminated nanocomposites. *Composites Part B: Engineering* **2018,** *147*, 33-41.